JOURNAL OF THE ROYAL SOCIETY Interface

Strength statistics of adhesive contact between a fibrillar structure and a rough substrate

Pankaj K Porwal and Chung Yuen Hui

J. R. Soc. Interface 2008 **5**, 441-448
doi: 10.1098/rsif.2007.1133

JOURNAL OF THE ROYAL SOCIETY Interface

J. R. Soc. Interface (2008) **5**, 441–448
doi:10.1098/rsif.2007.1133
Published online 20 August 2007

Strength statistics of adhesive contact between a fibrillar structure and a rough substrate

Pankaj K. Porwal[1,*] and Chung Yuen Hui[2]

[1]*Department of Civil Engineering, Indian Institute of Technology, Powai, Mumbai 400 076, India*
[2]*Department of Theoretical and Applied Mechanics, Cornell University, Ithaca, NY 14853, USA*

Equal distribution of load among fibrils in contact with a substrate is an important characteristic of fibrillar structures used by many small animals and insects for contact and adhesion. This is in contrast with continuum systems where stress concentration dominates interfacial failure. In this work, we study how adhesion strength of a fibrillar system depends on substrate roughness and variability of the fibril structure, which are modelled using probability distributions for fibril length and fibril attachment strength. Monte Carlo simulations are carried out to determine the adhesion strength statistics where fibril length follows normal or uniform distribution and attachment strength has a power-law form. Our results indicate that the strength distribution is Gaussian (normal) for both the uniform and the normal distributions for length. However, the fibrillar structure having normally distributed lengths has higher strength and lower toughness than one having uniformly distributed lengths. Our simulations also show that an increase in the compliance of the fibrils can compensate for both the substrate roughness and the attachment strength variation. We also show that, as the number of fibrils n increases, the load-carrying efficiency of each fibril goes down. For large n, this effect is found to be small. Furthermore, this effect is compensated by the fact that the standard deviation of the adhesive strength decreases as $1/\sqrt{n}$.

Keywords: fibrillar interfaces; adhesion strength statistics; random attachment strengths; random fibril lengths; surface roughness; size effects

1. INTRODUCTION

Fibrillar structures are used in nature for contact and adhesion by small animals and insects (Scherge & Gorb 2001; Arzt *et al.* 2003). For example, a tokay gecko's feet have approximately half a million fine hairs, called setae, which allow it to climb vertically and stick upside down on practically all surfaces. Each of the seta further splits into 200–1000 finer hairs with flat spatula-shaped tips having dimension of the order of a few hundred nanometres (Hiller 1968; Autumn *et al.* 2000).

Despite having less contact area for a given size of adhesive material, fibrillar interfaces can be stronger than flat interfaces made of the same material for several reasons: (i) in flat interfaces stress concentration dominates failure around the damage front, whereas fibrillar structures exhibit redundancy or equal sharing of loads or both, making them less sensitive to failure of a few fibrils (Glassmaker *et al.* 2005); (ii) stress concentration can be eliminated by employing fibrils with sufficiently small lateral dimensions (Gao *et al.* 2003; Gao & Yao 2004; Hui *et al.* 2004); (iii) fibrillar interfaces exhibit greater structural compliance, that is, individual fibrils can bend or buckle easily, allowing large numbers of fibrils to make good contact with rough substrates (Glassmaker *et al.* 2004); (iv) fibrillar structures can resist fouling by small particles (Hansen & Autumn 2005; Hui *et al.* 2006); and (v) in addition to the loss of surface energy, elastic energy stored in the fibrils is also lost during detachment (Jagota & Bennison 2002). Since the elastic energy stored in a fibril is directly proportional to its length, long fibrils are advantageous from an energy dissipation standpoint. However, there are limits to the length of fibrils since long fibrils can stick to each other to reduce surface energy—a condition called lateral collapse (Glassmaker *et al.* 2004; Greiner *et al.* 2007). Since collapsed fibrils do not make good contact with the substrate, lateral collapse is detrimental to adhesion.

Several researchers, motivated by these biological systems, have recently attempted to mimic the fibrillar architecture to attain enhanced adhesion (Geim *et al.* 2003; Sitti & Fearing 2003; Glassmaker *et al.* 2004; Gorb *et al.* 2006). Fabrication of synthetic structures with a high degree of hierarchy is still technologically challenging and most of the fibrillar adhesives

*Author for correspondence (pporwal@iitb.ac.in).

Received 10 June 2007
Accepted 30 July 2007

fabricated so far are either one- or two-level structures. The one-level structure typically consists of pillars having approximately uniform cross-sections and nominally flat tips (Geim *et al.* 2003; Sitti & Fearing 2003; Glassmaker *et al.* 2004; Gorb *et al.* 2006; Greiner *et al.* 2007). Although these structures typically show an increase in adhesion per unit area of *actual* contact, the overall adhesion was still less than that of a flat interface. The most successful designs typically involve two-level fibrillar structures consisting of an attachment element (e.g. mushroom-shaped element or thin plate) bonded to the nominally flat tip of the one-level structure (Gorb *et al.* 2006; Kim & Sitti 2006; Glassmaker *et al.* 2007). The strength and toughness of these structures are found to be considerably better than flat interfaces made of the same material.

There is a large literature on the contact mechanics and adhesion of fibrillar interfaces (Hui *et al.* 2007). Many of these works analysed the adhesive interaction of a single fibril in contact with a substrate. These works assume that all the material and geometrical parameters are deterministic, which tend to overestimate the adhesive strength of large fibrillar structures. For example, if van der Waals forces control adhesive interaction then even small variations in fibril length can significantly reduce the overall adhesion of the fibrillar structures. Thus, the detachment of a fibrillar surface consisting of n fibrils can occur at a force much less than np for small variations in fibril lengths, where p is the theoretical detachment strength of a single fibril obtained using a deterministic analysis. In a previous work, one of us had studied the effect of surface roughness or fibril length variation on adhesion (Hui *et al.* 2005), where the fibril lengths were assumed to obey a normal distribution with standard deviation σ_N. However, the adhesive strength p was assumed to be deterministic and was modelled using the Johnson–Kendall–Roberts theory (Johnson *et al.* 1971). Similar analysis was also carried on a hierarchical structure by Kim & Bhushan (2007).

In the work by Hui *et al.* (2005), only the mean strength of the fibrillar structure was determined. The problem of finding the probability distribution function of adhesive strength of the fibrillar structure, given the distribution function for length and tip attachment strength, is much more complicated and cannot be obtained based on the analysis employed by Hui *et al.* (2005). It is the intention of the present work to offer a solution to this problem.

2. DESCRIPTION OF MODEL

Consider a fibrillar surface with a very large number, n, of fibrils. Each fibril is endowed with an attachment element at its tip (e.g. a thin plate-like spatula). We assume that the attachment elements are of the same type, but can vary slightly in size and shape. In addition, the surface profile or roughness of the substrate directly underneath a particular attachment element can further influence the adhesive strength of the element. These effects on adhesion are local but can influence the overall adhesive strength if the fibril lengths are not equal. Owing to these unequal lengths, fibrils will support different loads and detach from the substrate in an asynchronous manner, leading to a reduction in adhesion. Surface roughness also enhances the effect of unequal fibril lengths, apart from affecting the attachment strength due to local variation in surface profile.

Since the surface roughness and fibril length variation have similar effects on the overall behaviour of the adhesive, we assume the substrate to be smooth and lump the roughness in the fibril length distribution. We assume that the attachment strength distributions account for both the local variation in substrate profile and the variation in the size and shape of the attachment element. In this model, both fibril length and fibril attachment strength are random quantities, that is, they vary from fibril to fibril.

2.1. Model for fibril length distribution

The lengths of the fibrils are assumed to be independent and identically distributed random variables. For concreteness, in this work the fibrils are assumed to follow either a normal or a uniform probability distribution. The density function for the normal distribution is

$$f_N(l) = \frac{1}{\sqrt{2\pi\sigma^2}} \exp\left\{-\frac{(l-l_0)^2}{2\sigma^2}\right\} \quad \text{for } -\infty < l < \infty, \tag{2.1}$$

where l_0 and σ are the mean and standard deviation, respectively. For the uniform distribution, the probability density function is

$$f_U(l) = \begin{cases} \dfrac{1}{l_{\max} - l_{\min}} & \text{for } l_{\min} \le l \le l_{\max}, \\ 0 & \text{otherwise}, \end{cases} \tag{2.2}$$

where $l_{\min}$ and $l_{\max}$ are the lower and upper limits for fibril lengths, respectively. The mean fibril length is $l_0 = (l_{\min} + l_{\max})/2$ and the standard deviation σ is $(l_{\max} - l_{\min})/\sqrt{12}$. We shall assume that the cross-sectional area and Young's modulus of the fibrils are deterministic, because small variations in these quantities do not significantly affect the adhesion. The effect of variations in fibril length and cross-sectional area on compliance is also small and thus it can also be assumed deterministic.

2.2. Model for adhesive interaction between an individual fibril and the substrate

Consider the following pull-off experiment which allows us to compute the strength statistics of the fibrillar adhesive. The upper end of the fibrillar structure is attached to a rigid surface. The fibrillar structure is brought into contact with a *smooth* substrate as shown in figure 1. Let d denote the separation between the rigid surface and the substrate. We first compress the fibrillar structure against the substrate, causing some or all of the fibrils to bend or to become slack, so that all the attachment elements are in contact with the substrate. We then increase d in discrete steps until pull-off occurs. The strength is defined as the maximum force supported

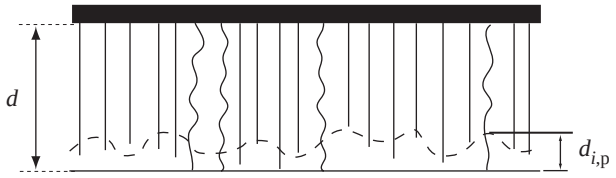

Figure 1. Schematic of the pull-off experiment, where d is the separation between the rigid surface and the substrate. The substrate is assumed to be smooth and $d_{i,p}$ denotes the range of attractive interaction of the ith fibril. Since fibrils have different lengths, during pull-off a fibril can be in compression, tension or out of the zone of attractive interaction with zero force.

by the adhesive in this process and will be defined as the pull-off force.

The interaction between the attachment element of a fibril and the substrate (shown to be smooth in figure 1, since the roughness is taken into account by the variations in length and attachment strength) is described below. Since the fibrils are long in comparison with their lateral dimensions, they are highly compliant under compressive loads (the role of compliance will be addressed later). Therefore, we will assume that they do not support any compressive load. Note that this approximation will have very little effect on the *maximum* pull-off force. Specifically, the force supported by a fibril, with length l_i, is zero when the separation d is less than its length, that is, when $d<l_i$. We call this a slack fibril. Mathematically, this condition is given as follows:

$$P_i(d) = 0 \quad \text{for } d - l_i < 0, \tag{2.3}$$

where P_i is the load on fibril i. As d increases, the slack in the ith fibril is removed until it becomes fully straight. We call this a non-slack fibril, which interacts adhesively with the substrate as long as its tip is within a distance of $d_{i,\mathrm{P}}$ away from the surface of the substrate. We call this region a 'zone of attractive interaction' (figures 1 and 2).

The force in a non-slack fibril increases linearly (since fibrils are elastic) until the attachment strength of the fibril, $P_{i,\max}$, is reached. After reaching this maximum, the force supported by the fibril remains constant as long as its tip lies in the zone of attractive interaction. Once the fibril tip is out of this zone, the force supported by it becomes zero (figure 2). Specifically,

$$P_i(d) = \begin{cases} k(d-l_i) & \text{for } 0 < k(d-l_i) \le P_{i,\max}, \\ P_{i,\max} & \text{for } P_{i,\max} < k(d-l_i) \le P_{i,\max} + kd_{i,\mathrm{p}}, \\ 0 & \text{otherwise}, \end{cases} \tag{2.4}$$

where k is the fibril stiffness. For a cylindrical fibril aligned perpendicular to the substrate such as those shown in figure 1, $k=EA/l_0$. For inclined fibrils, the expression for k can be found in Glassmaker *et al.* (2004).

The adhesive interaction model in this work is similar in spirit to the Dugdale–Barenblatt adhesion model (Dugdale 1960; Barenblatt 1962). Indeed, $P_{i,\max}$ and $P_{i,\max}d_{i,\mathrm{p}}$ can be identified as the fibril attachment strength and work to detach a fibril excluding the elastic

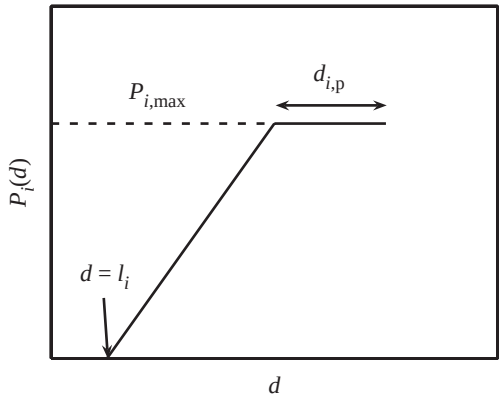

Figure 2. Adhesive interaction model, that is, force supported by an individual fibril, $P_i(d)$, versus separation between the rigid surface and substrate, d. Our model is similar in spirit to the Dugdale–Barenblatt model. Here $P_{i,\max}$ and l_i are the detachment strength and length of the ith fibril.

energy stored in the fibril just before detachment, respectively. Here, these quantities are random variables. To reduce the number of simulations, we assume that there is a positive correlation between $d_{i,\mathrm{p}}$ and $P_{i,\max}$. In the simulations below we assume that $d_{i,\mathrm{p}}=d_{i,\max}/2$, where $d_{i,\max}=P_{i,\max}/k$.

2.3. Model for adhesive strength of an individual fibril

As mentioned above, $P_{i,\max}$ is not deterministic. This is due to variations in local substrate geometry and attachment element. In the following, we assume that it obeys a power-law distribution with the cumulative probability distribution function

$$F_{\mathrm{P}}(p) = \begin{cases} 0 & \text{for } p \le 0, \\ (p/P_0)^{\rho} & \text{for } 0 < p \le P_0, \\ 1 & \text{for } p > P_0. \end{cases} \tag{2.5}$$

The probability density function, $\mathrm{d}F_{\mathrm{p}}/\mathrm{d}p$, is

$$f_{\mathrm{P}}(p) = \begin{cases} \rho p^{\rho-1}/P_0^{\rho} & \text{for } 0 < p \le P_0, \\ 0 & \text{otherwise}, \end{cases} \tag{2.6}$$

where P_0 and ρ are the intrinsic adhesive strength (or scale parameter) and the shape parameter, respectively. The scale parameter controls the magnitude and the shape parameter dictates the variability of the attachment strength; the lower the shape parameter the higher the variability. The mean and standard deviation of the tip attachment strength for power-law distribution are $\rho P_0/(1+\rho)$ and $P_0\sqrt{\rho/(\rho+2)-\rho^2/(\rho+1)^2}$, respectively.

2.4. Normalization

In the following, we normalize all forces by the intrinsic adhesive strength, P_0, lengths by the mean fibril length, l_0, and the stiffness of the fibrils by P_0/l_0. These

normalized variables are denoted by

$$\hat{k} = kl_0/P_0, \qquad \hat{P}_i = P_i/P_0,$$
$$\hat{P}_{i,\max} = P_{i,\max}/P_0, \qquad \hat{P} = P/nP_0, \tag{2.7}$$
$$\hat{d} = d/l_0, \qquad \hat{l}_i = l_i/l_0 \quad \text{and} \quad \hat{d}_{i,\mathrm{p}} = d_{i,\mathrm{p}}/l_0,$$

where P is the total force acting on the system, that is,

$$P \equiv \sum_{i=1}^{n} P_i(d). \tag{2.8}$$

Using these normalized variables, equations (2.4) and (2.8) become

$$\hat{P}_i(\hat{d}) = \begin{cases} \hat{k}(\hat{d}-\hat{l}_i) & \text{for } 0<\hat{k}(\hat{d}-\hat{l}_i)<\hat{P}_{i,\max}, \\ \hat{P}_{i,\max} & \text{for } \hat{P}_{i,\max}<\hat{k}(\hat{d}-\hat{l}_i)<\hat{P}_{i,\max}+\hat{k}\hat{d}_{\mathrm{p}}, \\ 0 & \text{otherwise,} \end{cases} \tag{2.9}$$

$$\hat{P}(\hat{d}) \equiv \frac{1}{n}\sum_{i=1}^{n} \hat{P}_i(\hat{d}). \tag{2.10}$$

The normalized pull-off force is

$$\hat{P}_{\text{pull-off}} = \max_{\hat{d}}\{\hat{P}(\hat{d})\}. \tag{2.11}$$

Note that a normalized pull-off force of unity is obtained when there is no variability.

3. MONTE CARLO SIMULATION

We performed Monte Carlo simulations to obtain the pull-off force distribution. All n fibrils have identical cross-sectional area and stiffness. However, their lengths and attachment strengths are random quantities obeying the probability distributions described in §2. The random lengths in each simulation are generated using the same probability distribution function, but the random length of an individual fibril is independent of the others. The same is true for the attachment strengths of fibrils. For the purpose of simulation, the fibrils are numbered as 1, …, i, …, n. These fibrils have lengths l_1, …, l_i, …, l_n and attachment strengths $P_{1,\max}$, …, $P_{i,\max}$, …, $P_{n,\max}$, which are generated using the inversion method. For example, random numbers with cumulative distribution function, F_X, are obtained using

$$X_i = F_X^{-1}(U_i), \tag{3.1}$$

where $U_i \sim U[0,1]$ is a uniform random number in [0,1]. The standard MATLAB random number generator function *rand* is used to generate these uniform random numbers.

In the simulations the normalized fibril stiffness, $\hat{k}$, shape parameter, ρ, and fibril length standard deviation, σ, and number of fibrils, n, are given. The following steps are performed for each replication:

(i) Random fibril lengths, l_1, …, l_i, …, l_n, and fibril attachment strengths, $P_{1,\max}$, …, $P_{i,\max}$, …, $P_{n,\max}$, are generated.
(ii) The initial separation between the rigid adhesive surface and substrate is taken to be less than the length of the shortest fibril so that all the fibril-tip attachment elements are in intimate contact with the substrate. At this stage all the fibrils are either bent or buckled, so the normalized force supported by the adhesive is $\hat{P}(\hat{d}) \equiv \sum_{i=1}^{n} \hat{P}_i(\hat{d}) = 0$.
(iii) The separation between the adhesive surface and the substrate is increased in discrete steps.
(iv) At each step the normalized load supported by each individual fibril is calculated using equation (2.9), which in turn is used to calculate the total normalized force supported by the adhesive (equation (2.10)).
(v) The separation between the adhesive surface and substrate is increased until all the fibril-tip attachment elements lose contact with the substrate and exit the zone of attractive interaction. At this stage, the load supported by the adhesive surface is again zero.
(vi) The maximum normalized force supported by the adhesive surface is the normalized pull-off force, $\hat{P}_{\text{pull-off}}$, of the adhesive for this replication.

Table 1. Values of the parameters used for simulation unless stated otherwise.

simulation parameter	value
number of fibrils, n	1000
power-law scale parameter, P_0	40 μN
mean fibril length, l_0	20 μm
fibril length standard deviation, σ	2.89 μm

The pull-off force distribution and the strength means and standard deviations are estimated using a total of 200 replications for a given set of parameters (k, ρ, σ, n).

4. NUMERICAL RESULTS

Table 1 shows typical parameters used for the simulations. These parameters are used unless stated otherwise. Simulations are performed for both the normal and the uniform distributions for fibril length. Figure 3 plots two realizations of the normalized force versus normalized displacement curves for different values of ρ. In all the curves, the initial slope is very small indicating that only few fibrils are bearing force (most are slack). As the separation between the adhesive and substrate, d, is increased, more and more fibrils are straightened and stretched. In this regime, the total force increases to a maximum. Also, as d increases the number of fibrils bearing force increases and hence the slope of each curve also increases. If the separation is increased further, the loss in force due to the pulling out of fibrils from the zone of attractive interaction exceeds the increase in force due to the straightening and stretching of fibrils, leading to a decrease in total force. Eventually, the force supported by the adhesive becomes zero when all the fibrils are pulled out of the zone of attractive interaction. Peaks in these curves (figure 3) correspond to pull-off forces. These peaks behave differently for fibrils with normal (exhibiting a distinct peak) and uniform (showing a much flatter peak) distributions for fibril length.

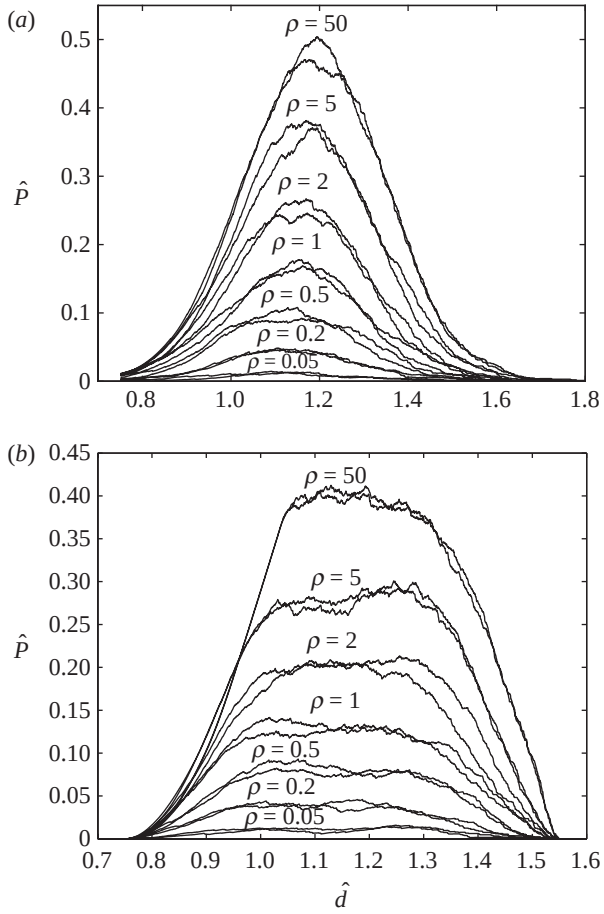

Figure 3. Normalized force supported by the adhesive surface, $\hat{P}$, versus normalized separation, $\hat{d}$, for (*a*) normal and (*b*) uniform distribution for fibril length. Two realizations (out of 200) are plotted for each value of the shape parameter, ρ. The value of k is 10 N m^{-1}.

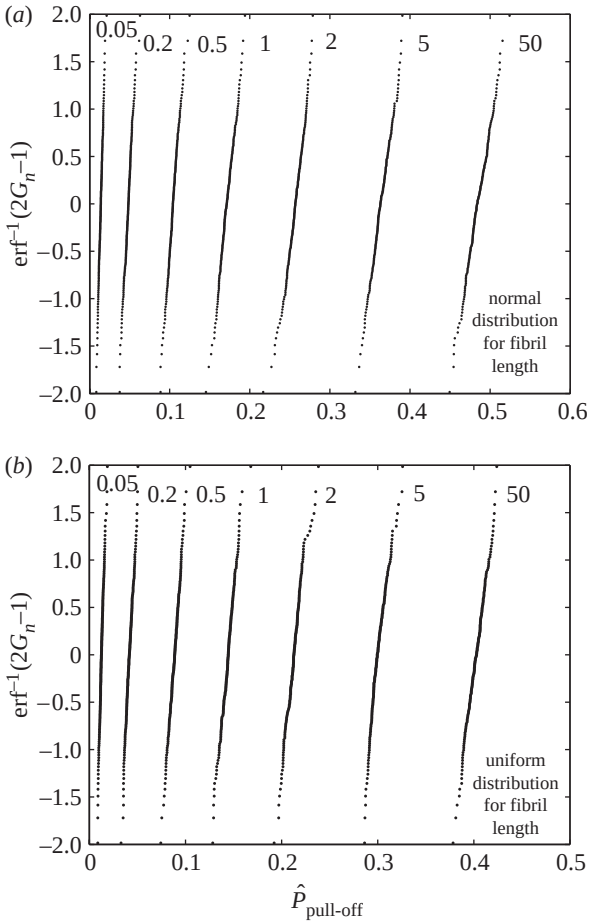

Figure 4. Cumulative probability distribution function, G_n, of normalized pull-off force, $\hat{P}_{\text{pull-off}}$, plotted on normal probability paper for (*a*) normal and (*b*) uniform distribution for fibril length. Here k=10 N m^{-1} and curves are labelled by the values of shape parameter, ρ. For the significance of $\mathrm{erf}^{-1}(2G_n-1)$, see Appendix A.

The normalized pull-off force increases with ρ (higher ρ means less variability of the fibril attachment strength). Near the peak, variation in force is more pronounced for all the cases (different ρ, normal or uniform distribution). In general, effective work of adhesion (the area under the force/displacement curve) is higher for the uniform length distribution. Note that the effective work of adhesion includes the elastic energy stored in the fibrils due to stretching, which can be much larger than the intrinsic work of adhesion.

Figure 4 plots the cumulative probability distribution, G_n, for the normalized pull-off force on normal probability paper. G_n is obtained numerically using the pull-off force data from the 200 replications of the Monte Carlo simulation. The linearity of the curves indicates that the pull-off force follows a normal distribution for fibrils with both the normal and the uniform length distributions.

Figure 5 shows how the mean normalized pull-off force depends on the normalized stiffness of the fibrils for different values of the shape parameter, ρ. As the stiffness decreases, that is, as the compliance increases, the mean pull-off force increases for all ρ. As expected, for a given fibril length standard deviation (approx. 10% of the mean length in figure 5), the pull-off force increases with decreasing stiffness and decreasing variability of the fibril attachment strength. This demonstrates that compliance can compensate for roughness and geometric irregularities of the attachments. The simplest way of increasing compliance is to use inclined or angled fibrils, as recently fabricated by Aksak *et al.* (2007).

Figure 6 plots the mean normalized pull-off force versus the normalized fibril stiffness for different fibril length standard deviations, σ. These curves show that the pull-off force decreases rapidly with fibril stiffness for high σ or rough surfaces. When the standard deviation for the length is 4% of the mean, the pull-off force decreases by more than 50% if $\hat{k}$ increases up to 20. These curves exhibit very similar behaviour for both the normal and the uniform distributions for fibril length, except that the mean pull-off force is slightly higher for the normal distribution.

4.1. Effect of number of fibrils on adhesive strength

We also explore how the number of fibrils affects the strength behaviour of the fibrillar structure. Figure 7*a*,*b* plots the mean and standard deviation of the

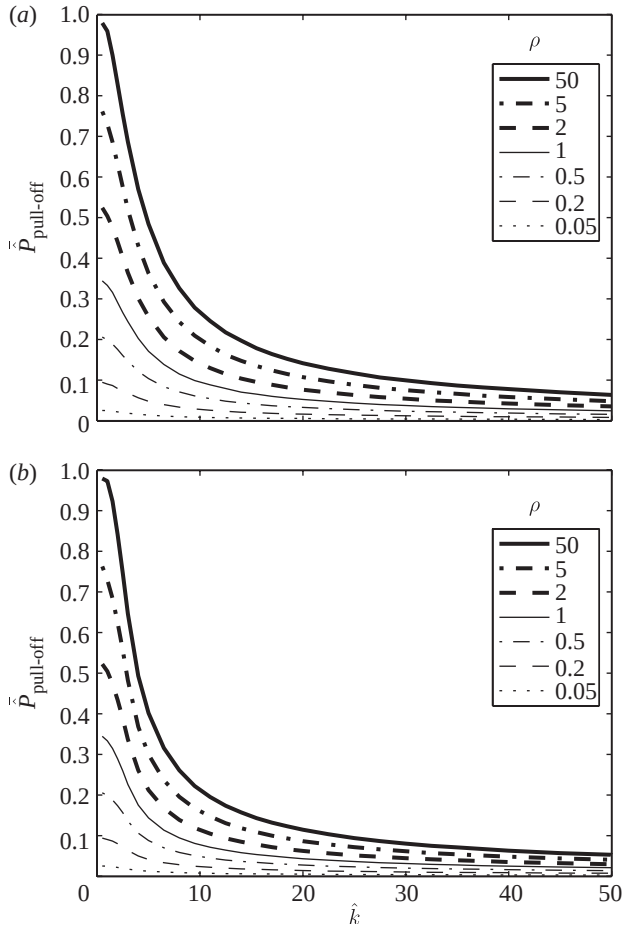

Figure 5. Mean normalized pull-off force, $\bar{\hat{P}}_{\text{pull-off}}$, versus normalized fibril stiffness, $\hat{k}$, for (*a*) normal and (*b*) uniform distribution for fibril length. The curves are for different values of ρ.

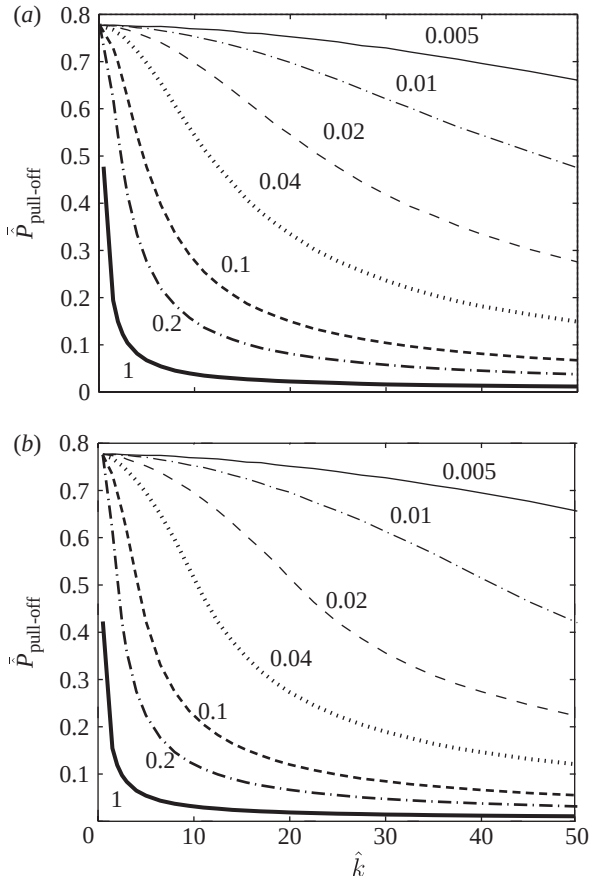

Figure 6. Mean normalized pull-off force, $\bar{\hat{P}}_{\text{pull-off}}$, versus normalized fibril stiffness, $\hat{k}$, for (*a*) normal and (*b*) uniform distribution for fibril length. Here $\rho=5$ and different curves in these figures correspond to different fibril length standard deviations labelled by the values of σ/l_0.

normalized pull-off force as a function of the number of fibrils n. Simulations are carried out only for fibrils having the normal distribution with $\rho=1$, 5 and $k=1$, $10\,\mathrm{N\,m^{-1}}$. Figure 7*a* shows that the mean normalized pull-off force, that is, the mean pull-off force per fibril, decreases as n increases. For $n\geq 10^3$, this decrease is very slow; numerically it seems to approach a limiting value. In other words, if one starts with a small number of fibrils then each fibril becomes less effective in bearing load as n increases, although the overall strength still goes up. However, for large n, this load-bearing efficiency is approximately independent of n; hence large fibril bundles are advantageous. In addition, the normalized standard deviation, $\sqrt{n}\gamma$, remains constant when plotted against n, indicating that variability of the pull-off force decreases as n increases according to

$$\gamma \propto 1/\sqrt{n}. \tag{4.1}$$

For a bundle where all the fibrils are of equal length but with attachment strength as a random variable, it is possible to show that this result follows from classical bundle theory (Daniels 1945; Phoenix 1974). For the problem studied in this work, in which the fibril length is also a random variable, we have not been able to prove this result mathematically except via simulation.

5. SUMMARY AND DISCUSSIONS

Monte Carlo simulation technique is used to study the adhesion statistics of a fibrillar structure consisting of a large number of fibrils. The lengths of the fibrils are random quantities and two different distributions (normal and uniform) are used to characterize them. In addition, the strength of the attachment element is also random and obeys a power-law distribution. Our results show that the pull-off force is approximately normally distributed. The mean pull-off force decreases rapidly with roughness, but this effect can be compensated by increasing the fibril compliance. We also studied the effect of number of fibrils in the adhesive patch and demonstrated numerically that the mean pull-off force per fibril decreases as the number of fibrils increases, for small n. These results are useful since they can be checked against experiments.

It might seem that the normality of the pull-off force distribution is a consequence of the central limit theorem. However, the random variables $\hat{P}_{\text{pull-off}} = \max_{\hat{d}}\left\{\hat{P}(\hat{d})\right\}$ occur at different values of the normalized separation, $\hat{d}$, for different replications. This prohibits the direct application of the central limit theorem. Indeed, the proof of this normality result is mathematically challenging even for a bundle

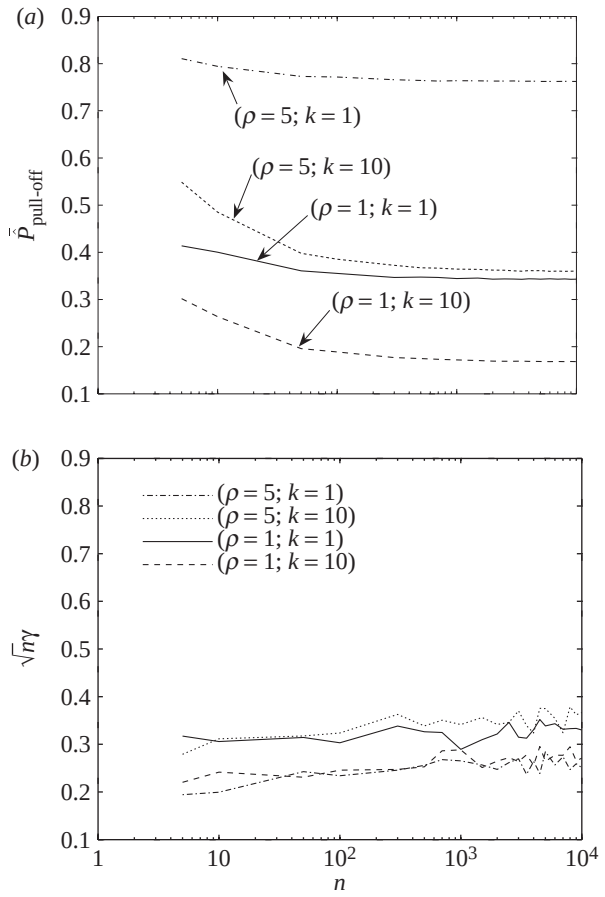

Figure 7. (*a*) Mean normalized pull-off force, $\bar{P}_{\text{pull-off}}$, versus number of fibrils, n, and (*b*) normalized standard deviation, $\sqrt{n}\gamma$, versus number of fibrils, n. Different curves are for different values of ρ and k.

consisting of parallel fibres of identical lengths as shown by Daniels (1945).

Although we have assumed specific distribution functions for the purpose of analysis, the technique presented in this work can be applied to any set of distributions. Indeed, experiments can be performed to determine the distribution function for the fibril attachment strength. For example, Huber *et al.* (2005) have studied the adhesive strength of a single spatula of a gecko and found that this is approximately 11 nN. However, the data in their paper are not presented in a form that would allow us to determine the distribution function. A limitation of this work is our assumption that the compressive preload is sufficiently large so that initially all the fibrils are in contact with the substrate. In reality, the degree of contact depends on the amount of compressive preload. Nevertheless, the conclusion of this paper is valid since we are interested in the maximum pull-off force. In practice, the pull-off force can be smaller and will depend on the preload, as demonstrated by Schargott *et al.* (2006), Aksak *et al.* (2007), Greiner *et al.* (2007) and Kim & Bhushan (2007).

The authors would like to thank Prof. S. L. Phoenix for his useful discussions and comments. C.Y.H. is supported by a grant from the National Science Foundation (CMS-0527785).

APPENDIX A

The cumulative distribution function for normal probability is of form

$$G_n = \frac{1}{2}\left[1 + \text{erf}\left(\frac{x - L_0}{\sqrt{2\sigma}}\right)\right],$$

where erf is the error function. We have plotted $\text{erf}^{-1}(2G_n - 1)$, where erf^{-1} is the inverse error function, against x; if we get a straight line, we can say that G_n is normally distributed.

REFERENCES

Aksak, B., Murphy, M. & Sitti, M. 2007 Adhesion of biologically inspired vertical and angled polymer microfiber arrays. *Langmuir* **23**, 3322–3332. (doi:10.1021/la062697t)

Arzt, E., Gorb, S. & Spolenak, R. 2003 From micro to nano contacts in biological attachment devices. *Proc. Natl Acad. Sci. USA* **100**, 10 603–10 606. (doi:10.1073/pnas.1534701100)

Autumn, K., Liang, Y. A., Hsieh, S. T., Zesch, W., Chang, W.-P., Kenny, T. W., Fearing, R. & Full, R. J. 2000 Adhesive force of a single gecko foot-hair. *Nature* **405**, 681–685. (doi:10.1038/35015073)

Barenblatt, G. I. 1962 The mathematical theory of equilibrium of crack in brittle fracture. *Adv. Appl. Mech.* **7**, 55–129.

Daniels, H. E. 1945 The statistical theory of the strength of bundles of threads I. *Proc. R. Soc. A* **183**, 405–435. (doi:10.1098/rspa.1945.0011)

Dugdale, D. S. 1960 Yielding of steel sheets containing slits. *J. Mech. Phys. Solids* **8**, 100–104. (doi:10.1016/0022-5096(60)90013-2)

Gao, H. & Yao, H. 2004 Shape insensitive optimal adhesion of nanoscale fibrillar structures. *Proc. Natl Acad. Sci. USA* **101**, 7851–7856. (doi:10.1073/pnas.0400757101)

Gao, H., Ji, B., Jaeger, I. L., Arzt, E. & Fratzl, P. 2003 Materials become insensitive to flaws at nanoscale: lessons from nature. *Proc. Natl Acad. Sci. USA* **100**, 5597–5600. (doi:10.1073/pnas.0631609100)

Geim, A. K., Dubonos, S. V., Grigorieva, I. V., Novoselov, K. S., Zhukov, A. A. & Shapoval, S. Y. 2003 Microfabricated adhesive mimicking gecko foot-hair. *Nat. Mater.* **2**, 461–463. (doi:10.1038/nmat917)

Glassmaker, N. J., Jagota, A., Hui, C.-Y. & Kim, J. 2004 Design of biomimetic fibrillar interfaces. 1. Making contact. *J. R. Soc. Interface* **1**, 22–33. (doi:10.1098/rsif.2004.0004)

Glassmaker, N. J., Jagota, A. & Hui, C.-Y. 2005 Adhesion enhancement in a biomimetic fibrillar interface. *Acta Biomater.* **1**, 367–375. (doi:10.1016/j.actbio.2005.02.005)

Glassmaker, N. J., Jagota, A., Hui, C.-Y., Noderer, W. L. & Chaudhury, M. K. 2007 Crack trapping for enhanced adhesion. *Proc. Natl Acad. Sci. USA* **104**, 10 786–10 791. (doi:10.1073/pnas.0703762104)

Gorb, S., Varenberg, M., Peressadko, A. & Tuma, J. 2006 Biomimetic mushroom-shaped fibrillar adhesive microstructure. *J. R. Soc. Interface* **4**, 271–275. (doi:10.1098/rsif.2006.0164)

Greiner, C., del Campo, A. & Arzt, E. 2007 Adhesion of bioinspired micropatterned surfaces: effects of pillar radius, aspect ratio, and preload. *Langmuir* **23**, 3495–3502. (doi:10.1021/la0633987)

Hansen, W. R. & Autumn, K. 2005 Evidence of self-cleaning in gecko setae. *Proc. Natl Acad. Sci. USA* **102**, 385–389. (doi:10.1073/pnas.0408304102)

Hiller, U. 1968 Studies on fine structure and function of the digital setae of lizards. *Z. Morph. Tiere* **62**, 307–362. (doi:10.1007/BF00401561)

Huber, G., Gorb, S., Spolenak, R. & Arzt, E. 2005 Resolving the nanoscale adhesion of individual gecko spatulae by atomic force microscopy. *Biol. Lett.* **1**, 2–4. (doi:10.1098/rsbl.2004.0254)

Hui, C.-Y., Glassmaker, N. J., Tang, T. & Jagota, A. 2004 Design of biomimetic fibrillar interfaces. 2. Mechanics of enhanced adhesion. *J. R. Soc. Interface* **1**, 35–48. (doi:10.1098/rsif.2004.0005)

Hui, C.-Y., Glassmaker, N. J. & Jagota, A. 2005 How compliance compensates for surface roughness in fibrillar adhesion. *J. Adhesion* **81**, 699–721. (doi:10.1080/00218460500187673)

Hui, C.-Y., Shen, L., Jagota, A., & Autumn, K. 2006 Mechanics of anti-fouling or self-cleaning in gecko. In *Proc. 29th Annual Meeting of the Adhesion Society*, pp. 29–31. Blacksburg, VA: Adhesion society, Inc.

Hui, C.-Y., Jagota, A., Shen, L., Rajan, A., Glassmaker, N. & Tang, T. 2007 Design of bio-inspired fibrillar interfaces for contact and adhesion—theory and experiments. *J. Adhes. Sci.Technol.* **21**, 1259–1280. (doi:10.1163/156856107782328362)

Jagota, A. & Bennison, S. J. 2002 Mechanics of adhesion through a fibrillar microstructure. *Integr. Comp. Biol.* **42**, 1140–1145. (doi:10.1093/icb/42.6.1140)

Johnson, K. L., Kendall, K. & Roberts, A. D. 1971 Surface energy and the contact of elastic solids. *Proc. R. Soc. A* **324**, 301–313. (doi:10.1098/rspa.1971.0141)

Kim, T. W. & Bhushan, B. 2007 The adhesion analysis of multi-level hierarchical attachment system contacting with a rough surface. *J. Adhes. Sci. Technol.* **21**, 1–20. (doi:10.1163/156856107779976097)

Kim, S. & Sitti, M. 2006 Biologically inspired polymer microfibers with spatulate tips as repeatable fibrillar adhesives. *Appl. Phys. Lett.* **89**, 26 911–26 913. (doi:10.1063/1.2424442)

Phoenix, S. L. 1974 Probabilistic strength analysis of fiber bundle structures. *Fiber Sci. Technol.* **7**, 15–31. (doi:10.1016/0015-0568(74)90003-7)

Schargott, M., Popov, V. L. & Gorb, S. 2006 Spring model of biological attachment pads. *J. Theor. Biol.* **243**, 48–53. (doi:10.1016/j.jtbi.2006.05.023)

Scherge, M. & Gorb, S. 2001 *Biological micro- and nano-tribology: nature's solutions*, ch. 44, pp. 139–147. Berlin, Germany: Springer.

Sitti, M. & Fearing, R. S. 2003 Synthetic gecko foot-hair micro/nano-structures as dry adhesives. *J. Adhes. Sci. Technol.* **17**, 1055–1073. (doi:10.1163/156856103322113788)